The International Journal of Advanced Manufacturing Technology (2019) 102:2695–2708
https://doi.org/10.1007/s00170-019-03379-w

ORIGINAL ARTICLE

Improving the machining efficiency of electrochemical micromachining with oscillating workpiece

Yufeng Wang [1] · Yongbin Zeng [2] · Wenwu Zhang [1]

Received: 7 August 2018 / Accepted: 21 January 2019 / Published online: 4 February 2019

Abstract

To enhance the machining efficiency of electrochemical micromachining (EMM), the low-frequency sinusoidal oscillating motion was applied to the workpiece, while the tool electrode moved in controlled trajectory. Mathematical model for the material removal rate (MRR) and the pressure in the interelectrode gap were derived. The mechanisms of enhancing the mass transport in the interelectrode gap induced by the oscillating workpiece during EMM have been analyzed, based on the variation of pressure in the interelectrode gap. An experimental setup has been developed for EMM. Experiments were conducted to investigate the influences of a vibrating amplitude and frequency on the machining efficiency, stability, and achievable maximum feeding rate of the tool electrode. The results indicated that a larger vibrating amplitude and a proper frequency were suitable for obtaining a higher material removal rate during EMM. The highest feeding rate of 0.3 μm/s has been obtained utilizing oscillating workpiece during the machining of microgrooves. Both the theoretical and the experimental results indicated that the oscillating workpiece during EMM was beneficial to improving the machining efficiency. Finally, microstructures with the circular profiles were processed using EMM, by a tool electrode feeding rate of 0.3 μm/s and the workpiece oscillation with the amplitude of 0.5 μm and frequency of 60 Hz.

Keywords Electrochemical micromachining oscillation · Interelectrode gap · Machining efficiency · Stability

1 Introduction

Miniaturization of components and systems is increasingly taking place, and is revolutionizing such areas as automobile, aerospace, microelectronics, medical devices, and optics engineering. The utilization of micro-products and microelectromechanical systems (MEMS) in various products could boost the energy efficiency and intelligence within limited space [1]. A wide spectrum of techniques for micromachining has been developed to meet the demand of miniaturization of components made from metals or semiconductors, including micro-mechanical turning, lithography-based processes, laser micromachining, electro-discharge machining (EDM), focused ion beam machining (FIB), and electrochemical micromachining (EMM) [2].

EMM proves to be a promising technique for fabricating tiny microstructures without introducing residual stresses and heat-affected zone, regardless of the mechanical and thermal properties of the workpiece materials. EMM has been increasingly employed in the micromachining area. An accuracy of micrometer or sub-micrometer scale could be obtained by applying ultrashort voltage pulses in EMM [3]. Kock et al. [4] studied the effects of pulse duration on the machining accuracy of EMM with ultrashort voltage pulses. Ahn et al. [5] utilized EMM for micro-drilling process, and high-quality micro-holes of 8 μm in diameter were drilled on 304 stainless steel foils of 20 μm in thickness. Kim et al. [6] proposed micro-electrochemical milling for processing three-dimensional microstructures. Liu et al. [7] fabricated 3D complex microstructures taking the advantage of layer-by-layer micro-electrochemical milling. Mithu et al. [8] studied the

✉ Yufeng Wang
wangyufeng@nimte.ac.cn

Yongbin Zeng
biny@nuaa.edu.cn

Wenwu Zhang
zhangww@nimte.ac.cn

[1] Institute of Advanced Manufacturing Technology, Ningbo Institute of Materials Technology and Engineering, Chinese Academy of Science, Ningbo 315201, Zhejiang, China

[2] College of Mechanical and Electrical Engineering, Nanjing University of Aeronautics and Astronautics, Nanjing 210016, Jiangsu, China

applied frequency and duty cycle in electrochemical micro-drilling process. Ghoshal and Bhattacharyya [9] proposed a sinking and milling method for generating micro-channel by EMM.

One of the key issues in EMM is the high-efficiency mass transport in the interelectrode gap of micrometer or sub-micrometer scale. Accumulation of the electrolytic products in the interelectrode gap may affect the stability of EMM and decrease the machining efficiency. In general, the diffusion of electrolytic products away from the interelectrode gap is mainly dominated by the concentration gradient, and a diffusion layer on the workpiece surface is formed [10].Also, the fresh electrolyte is difficult to be refreshed at the interface of electrochemical reactions. The low efficiency of mass transport in the micro-interelectrode gap has posed difficulties in improving the machining efficiency and stability of EMM. Previous study has mentioned that the accumulation of electrolytic products could decrease the electrolyte conductivity across the machining area, resulting in low machining efficiency of EMM [11]. The transportation rate of dissolution products also affects the distribution of current density on the anode surface and the surface quality of the machined area.

To enhance the mass transport in the micro-interelectrode gap, an oscillation or rotation has been introduced to the tool electrode or the workpiece. Ebeid et al. [12] demonstrated the improvement of machining accuracy for EMM hybridized with low frequency vibrations of tool electrode. Munda et al. [13] applied tool vibration frequency of 100 Hz in EMM to reduce the micro-spark and stray current–affected area. Bhattacharyya et al. [14] concluded that a vibrating micro-tool with Hertz (Hz) range frequency could improve the material removal rate (MRR) and machining precision in EMM. Hewidy et al. [15] theoretically studied the performance of EMM assisted by low frequency vibrations of tool electrode. Yang et al. [16] resolved the problems with electrolyte diffusion during EMM by using ultrasonic vibrated semi-cylindrical tool, and the electrolyte diffusion in the flow space was improved. Zeng et al. [17] employed the micro-vibration of cathode wire electrode to enhance mass transport in microwire electrochemical machining. Natsu et al. [18] applied ultrasonic vibration to the tool electrode in EMM and experimentally investigated the effects of vibration direction, amplitude, and the tool feed rate on the replicating accuracy and processing speed. Xu and Pan [19] showed that the localization of EMM could be increased making use of a vibrating tool electrode. Wang et al. [20] indicated that the micro-tool vibration could promote the renew of electrolyte and concluded that a low frequency and small amplitude vibration significantly improve processing stability while using a wire electrode. Ghoshal and Bhattacharyya [21] reported that vibration of micro-tool with a very small amplitude improved the stability of EMM due to the increased flow of electrolyte. Wang et al. [22] introduced ultrasonic vibration to the micro-tool in electrochemical micro-hole drilling, and the machining speed and maximum depth of the machined micro-holes increased obviously. Ghoshal and Bhattacharyya [23] revealed that a low amplitude and medium frequency vibration of micro-tool could improve machining conditions and machining current. Fan and Hourng [24] also utilized a rotational tool electrode to extract insoluble sludge while electrochemical drilling of deep micro-holes. However, further studies are still needed to investigate the mechanisms of mass transport in the sub-micrometer-sized interelectrode. Few studies investigated the influences of the workpiece vibrating frequency and amplitude on the machining efficiency and stability. The mathematical model of the pressure across the front interelectrode gap during EMM was not derived either.

To enhance the mass transport across the interelectrode gap, this paper introduced an oscillating motion to the workpiece. Compared with previous studies in which the tool vibrated, the sinusoidal oscillation with the controlled amplitude and frequency has been applied to the workpiece in this paper. The workpiece vibration could avoid the dynamic deformation of the sub-micro-tool electrode due to the mounting or geometry error, which in turn deteriorates the stability and accuracy of EMM. Moreover, the dynamic motion of the workpiece could directly increase the kinetic energy of the electrolytic products at the workpiece/electrolyte interface, which could improve the diffusion efficiency of the electrolytic products towards the bulk electrolyte. The mathematical model of material removal rate and the pressure in the interelectrode gap induced by the oscillating workpiece have been derived. The enhancing mechanisms of mass transport across the interelectrode gap with oscillating workpiece were explained as well. Micro-channels were processed by EMM with an oscillating workpiece and the lateral feeding of micro-tool electrode. Moreover, influences of the vibrating parameters including a vibrating amplitude and frequency on the machining current, side gap, stability, and the maximum feeding rate were investigated, experimentally.

2 Mathematical modeling of EMM with the oscillating workpiece

2.1 Effects of the workpiece oscillation on the MRR

In EMM, the workpiece, served as the anode, is removed by anodic dissolutions. Electrolytic products are generated at the interface of electrolyte and workpiece. As illustrated in Fig. 1, the front interelectrode gap varies according to the feeding of the tool electrode and the sinusoidal oscillating motion of the workpiece, when a cylindrical micro-

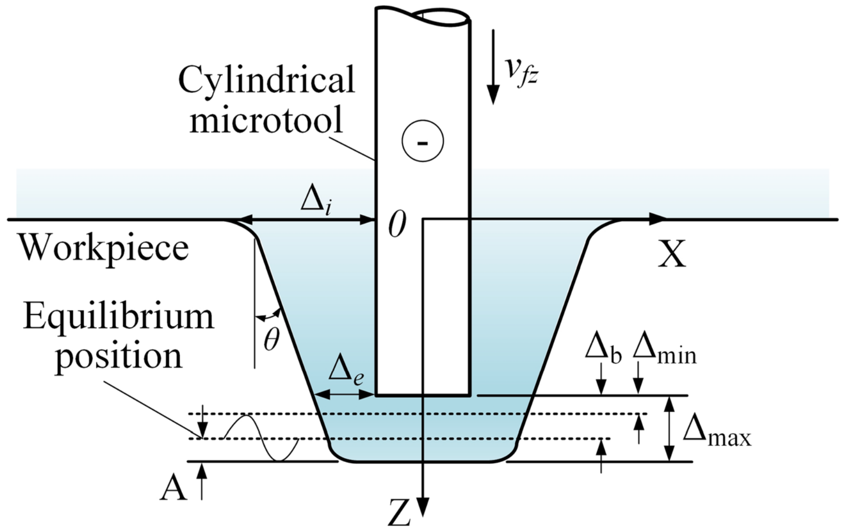

Fig. 1 Schematic diagram of the variation of the interelectrode gap during electrochemical micromachining with the oscillating workpiece

tool is used as the cathode. The oscillating workpiece provides EMM process with the following advantages:

(1) The vibrating workpiece could generate variation in the front gap without affecting the sub-micro-tool electrode.
(2) As the diffusion efficiency of the electrolytic products increased due to the improved kinetic energy at the machining area, the exchange rate of reaction ions at the workpiece/electrolyte interface could be increased, thus the current density and machining efficiency on the machining area could be improved [23].
(3) The variation of electrolyte pressure in the interelectrode gap and material removal rate caused by the workpiece vibration enhances the mass transport in the interelectrode gap.

A piezo actuator provides the oscillating motion of the workpiece in simple harmonic motion mode. The displacement of the workpiece is expressed by [15]:

$$z(t) = A\sin(2\pi ft + \varphi) \tag{1}$$

where A is the oscillation amplitude, f is the oscillation frequency, and φ is the phase angle ($\varphi = 0$). The oscillation velocity of the workpiece, $v(t)$, is expressed as:

$$v(t) = \frac{\partial z(t)}{\partial t} = 2\pi Af\cos(2\pi ft) \tag{2}$$

Compared with the EMM process in which the tool electrode feeds towards the workpiece at a constant rate, the instantaneous feed rate of the tool electrode relative to the workpiece varies with the oscillating workpiece. The instantaneous feeding rate of the tool electrode (v_f) is the sum of constant feed rate (v_{fz}) and the oscillation velocity of the workpiece, $v(t)$, that is

$$v_f = v_{fz} + 2\pi Af\cos(2\pi ft) \tag{3}$$

Supposed that EMM is in the state of equilibrium, based on Ohm's law and Faraday's Law, the front equilibrium interelectrode gap could be expressed as [24]:

$$\Delta_b = \eta\omega\sigma\frac{U-\delta E}{v_{fz}} = \frac{E\sigma\eta}{F\rho_m} \tag{4}$$

where η is the current efficiency, ω is the volumetric electrochemical equivalent of the workpiece materials, σ is the electrolyte conductivity, U is the applied voltage between the two counter electrodes, δE is the overall over-potential, F is the Faraday's constant, and ρ_m is the density of workpiece. As illustrated in Fig. 1, the front interelectrode gap (Δ) changes repeatedly with an oscillation of the workpiece. The instantaneous front interelectrode gap could be calculated by the following equation:

$$\Delta = \Delta_b + A\sin(2\pi ft) \tag{5}$$

where Δ_b is the equilibrium interelectrode gap. Therefore, the front interelectrode gap changes periodically in the range from $\Delta_{min} = \Delta_b - A$ to $\Delta_{max} = \Delta_b + A$. The current density ($j$) on the workpiece surface is given by [15]:

$$j = \frac{\sigma(U-\delta E)}{\Delta_b + A\sin(2\pi ft)} \tag{6}$$

Based on the Faraday's law, the material removal rate (MRR), as a function of machining time t, could be expressed by the following equation:

$$MRR = \frac{EI}{\eta\rho_m F} = \frac{\sigma EA(U-\delta E)}{\eta\rho_m F[\Delta_b + A\sin(2\pi ft)]} \tag{7}$$

Hence, the material removal rate of EMM varies periodically with the oscillating workpiece. As shown in Fig. 2, it could be concluded that the material removal rate increases with the oscillating amplitude of the workpiece. An oscillating frequency of 50 Hz, equilibrium interelectrode gap of 1 μm, and voltage of 4 V were used. In addition, the material removal rate increased as the workpiece moves upward (close towards the tool electrode) and decreased while the workpiece moves downward (far from the tool electrode).

2.2 Effects of oscillation on the pressure in the interelectrode gap

To study the mechanical effect that the oscillating workpiece imparts to the electrolyte across the front interelectrode gap, a fluid micro-cell was used, as shown in Fig. 3. The immersed depth of the micro-tool electrode is h, the distance between the end of the micro-tool electrode and the micro-cell is z, and the height of the micro-cell is dz. Then, the oscillating motion of the micro-cell could be expressed as the following expression [25]:

$$z = A\sin 2\pi f\left(t - \frac{z}{c}\right) \tag{8}$$

where c is the wave traveling speed in the electrolyte medium. Then, the acceleration of the micro-cell is given by

$$a = \frac{\partial^2 z}{\partial t^2} = -4A\pi^2 f^2 \sin 2\pi f\left(t - \frac{z}{c}\right) \tag{9}$$

Assuming that the cross-sectional area of the micro-cell is s, the pressure acting on the upper and lower surface of the micro-cell are P and $P + dP$, respectively. The forces acting on the micro-cell could be expressed as:

$$Ps + d(mg) - (P + dP)s = (\rho_e s dz)a \tag{10}$$

where ρ_e is the density of electrolyte, m is the mas of the micro-cell, and g is the gravitational acceleration.

$$dP = \left[\rho_e g + 4\pi^2 f^2 \rho_e A \sin 2\pi f\left(t - \frac{z}{c}\right)\right] dz \tag{11}$$

When $z = 0$, $P = P_0$, where P_0 is the atmospheric pressure on the electrolyte surface. Therefore, the pressure in the front interelectrode gap could be calculated by Eq. 11 and the boundary conditions:

$$P = \rho_e g(h + z) + 2\pi f A \rho_e c \cos 2\pi f\left(t - \frac{z}{c}\right) + P_0 \tag{12}$$

Based on Eq. 12, it could be concluded that the pressure in the interelectrode gap alters much faster under a higher oscillating frequency. As shown in Fig. 4, the pressure in the interelectrode gap changes around the atmospheric pressure (1.0×10^5 Pa). Moreover, the deviation from the atmosphere pressure increases as the oscillating frequency increases. Obviously, the fresh electrolyte would be pump into the machining gap under the pressure that is smaller than the atmospheric pressure. Contrarily, both electrolytic products and the electrolyte are pushed away from the narrow interelectrode gap under pressure difference, while the pressure in the interelectrode gap is smaller than that on the electrolyte surface. Therefore, the mass transport across the interelectrode gap is enhanced, which would be enhanced by increasing oscillating frequency. Under a constant oscillating frequency of 50 Hz, the difference between the pressure in the interelectrode gap and that on the electrolyte surface is increased as the

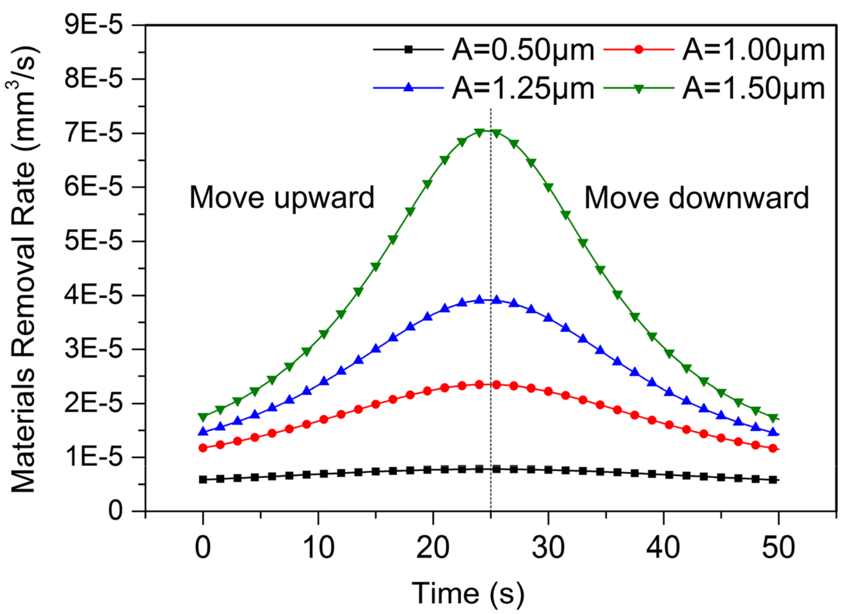

Fig. 2 Variation of the material removal rate with the workpiece oscillation amplitude during EMM

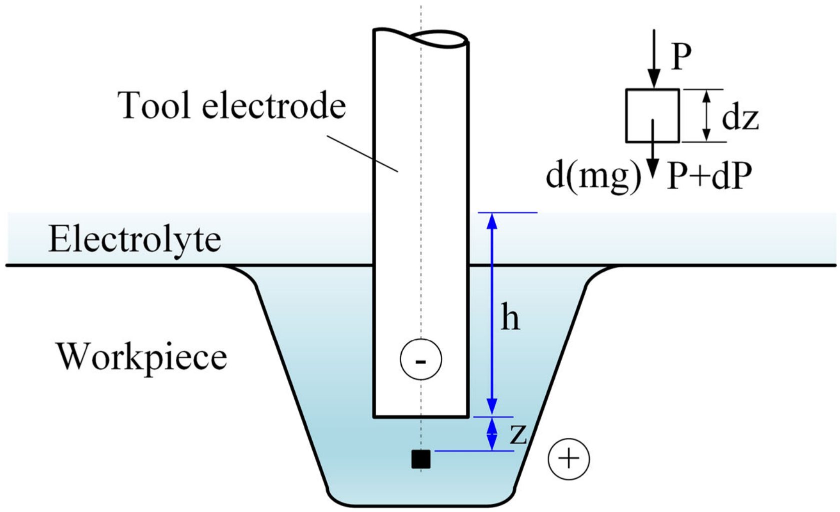

Fig. 3 Schematic diagram of pressure in the interelectrode gap during EMM

oscillating amplitude improves, as shown in Fig. 5. Under a larger difference in pressure, the flow of the electrolyte could be strengthened; thus, the mass transport in the interelectrode gap could be improved with a larger oscillating amplitude and frequency. The increased oscillating frequency also improves the changing frequency of the pressure in the interelectrode gap, which has an effect of stirring on the electrolyte in the machining area during EMM. Thus, the uniformity of electrolytic product distribution in the narrow interelectrode gap could also be improved, which, in turn, improves the uniformity of current density distribution in the machining area.

2.3 Mechanisms of mass transport enhancement by the oscillating workpiece

The above analysis pointed out that the variation of pressure in the interelectrode gap generated by the oscillating workpiece during EMM could enhance the flow of electrolyte and electrolytic products in the interelectrode gap. Moreover, material removal rate also varies with oscillating workpiece. Based on Eqs. 8 and 13, it could be concluded that both the pressure in the interelectrode gap and the volume of the generated electrolytic products increased as the workpiece moves upward (close towards the tool electrode), while the interelectrode gap is decreased. The quantity of generated electrolytic products in the machining area also increases. With a synchronous improvement of electrolyte pressure in the interelectrode gap, the electrolytic products could be pushed away from the interelectrode gap with a flow of electrolyte under higher pressure in the interelectrode gap, as illustrated in Fig. 6a. In the case of the workpiece oscillated in the backward direction (far from the tool electrode), the interelectrode gap increases and the pressure in the interelectrode gap reduced to a value lower than the atmospheric

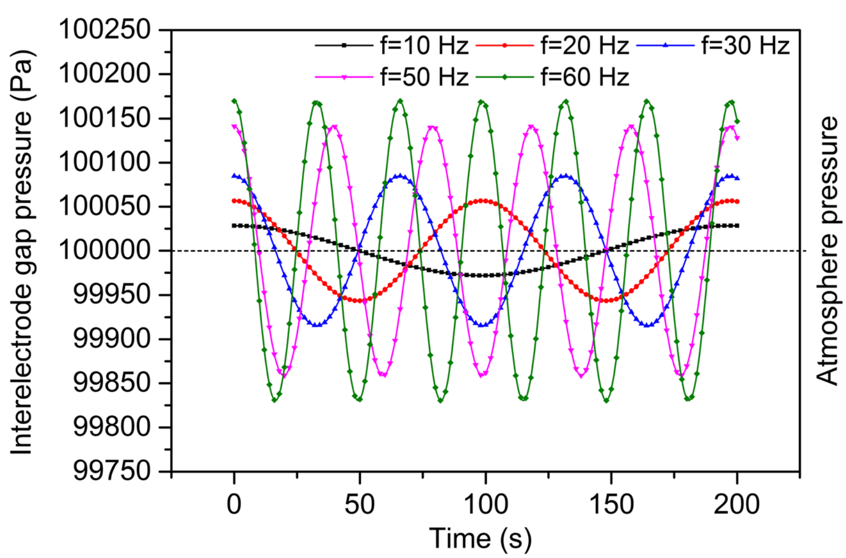

Fig. 4 Variation of pressure in the interelectrode gap with workpiece oscillating frequency during EMM

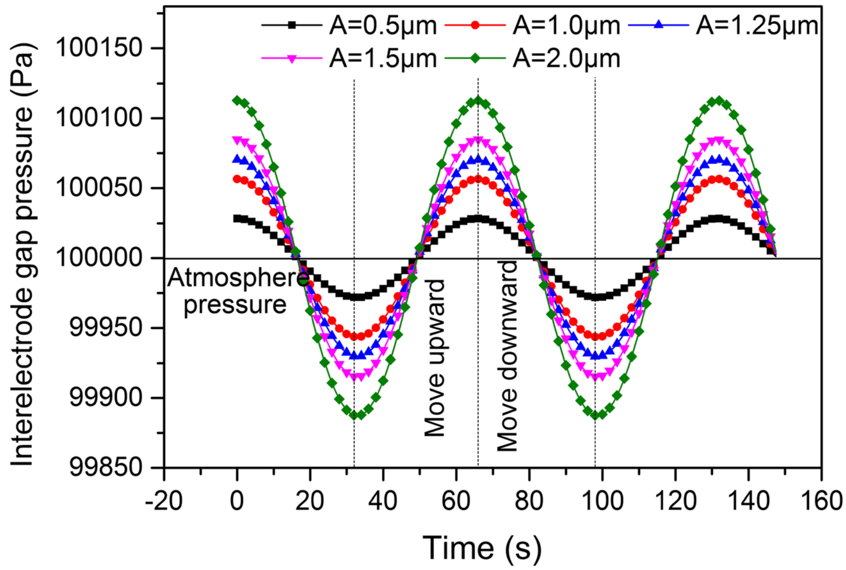

Fig. 5 Variation of pressure in the interelectrode gap with a workpiece oscillating amplitude during EMM

pressure. Meanwhile, the volume of the generated electrolytic products decreases as the fresh electrolyte pushed into the interelectrode gap during EMM, as illustrated in Fig. 6b. Hence, the proportion of electrolytic products in the machining area is decreased, and the electrolyte in the interelectrode gap is renewed, to some extent. As the discussions above, the electrolytic products could be removed from the machining area, and the electrolyte in the interelectrode gap could be refreshed in 1 cycle of oscillation motion. Therefore, the mass transport in machining area is enhanced effectively by applying oscillation motion to the workpiece during EMM.

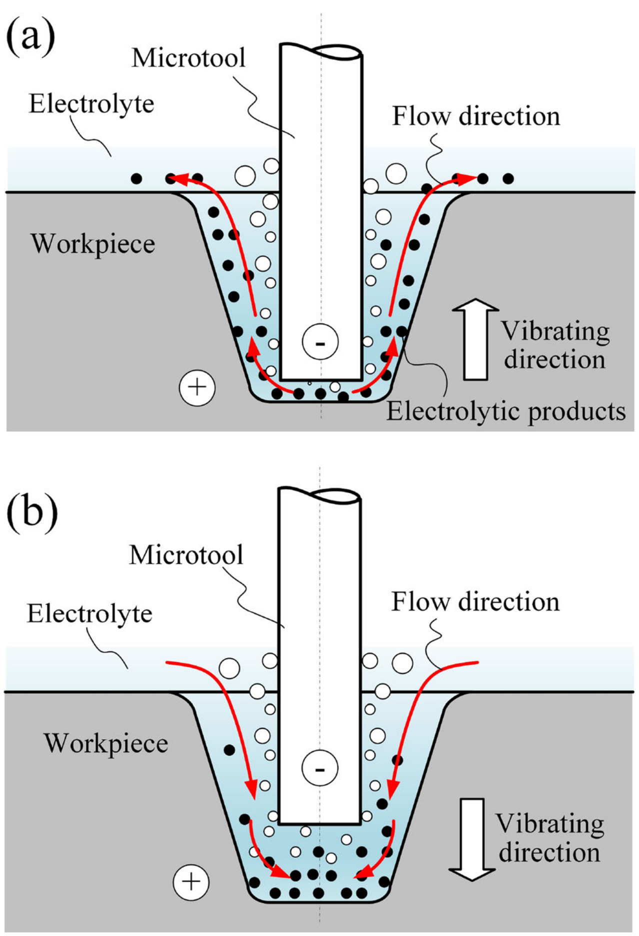

Fig. 6 Enhancement of mass transport in the interelectrode gap by the oscillating workpiece during EMM. The workpiece moves upward (close towards the tool electrode) (**a**), the workpiece moves downward (far from the tool electrode) (**b**)

3 Experimental

An experimental setup for electrochemical micromachining has been developed, as shown in Fig. 7, which contains macro and micro precision movement systems, vibration-proof base (TMC), pulse voltage power, electrolyte circulation system, electric current monitoring system, and control unit. The three-dimensional macro movement system, composed of three linear stages (M511.DG, PI), could provide the tool electrode with the controlled feeding trajectory in high speed, with a resolution of 0.1 μm. In comparison, the three-dimensional piezo transducer (P561.3CD, PI) could allow the workpiece to feed and to oscillate with a resolution of 0.8 nm. A tool electrode was fixed to a spindle (NR-2551, NAKANISHI) that is attached to the three-dimensional macro movement system. As shown in Fig. 8, the tool electrodes with cylinder end of 0.65 μm in diameter have been prepared by electrochemical etching using vibrating electrolyte membrane method [26]. The tool electrode was made of tungsten to avoid the deformation during EMM with its good comprehensive mechanical properties. A solution of sulfuric acid (H_2SO_4) was used as the electrolyte. The workpiece made

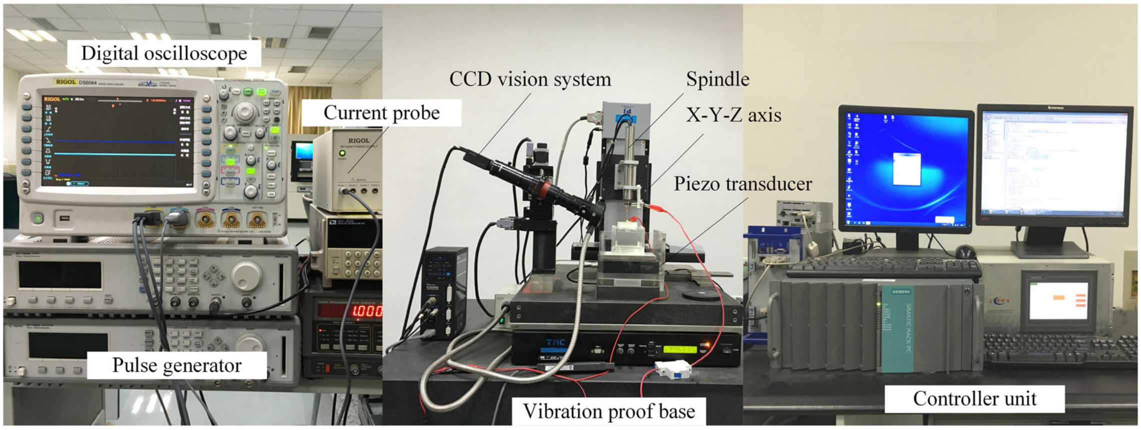

Fig. 7 Experimental setup for EMM with the oscillating workpiece

of super alloy (GH4169) was immersed in the electrolyte within the electrolytic cell. A pulse generator (81110A, Keysight) provides the pulse voltage of nanosecond duration between the tool electrode and workpiece. The experimental conditions are listed in Table 1. The profiles of the processed microstructures were measured by an atomic force microscopy (Dimension Edge, Bruker).

Microgrooves have been processed layer-by-layer with each layer thickness of 0.1 μm, and two layers were applied in processing microgrooves. The machining precision, presented by the side gap (Δ_s), was calculated by $\Delta_s = (w - d)/2$, where w is the width of the processed microgroove, and d is the tool electrode end diameter. Also, the machining efficiency was evaluated by the maximum feeding rate of the tool electrode during EMM. A higher maximum feeding rate of the tool electrode means a higher machining efficiency.

During EMM, the physical contact between the tool electrode and workpiece should be avoided in case of the damage to the tool electrode end caused by electric short circuit or instant crash. A method should be employed to monitor the occurrence of the electric short circuit. If an electric short circuit was detected, the feeding of the workpiece should be suspended immediately, and then be retreated at an initial interelectrode gap along the feeding direction. Both the voltage and electric current signal between the two polarities were monitored by a digital oscilloscope (DS6000, RIGOL). As shown in Fig. 9, it could be observed that the interelectrode voltage dropped, while the electric current increased abruptly, when an electric short circuits happened. By monitoring the variation of voltage and electric current, the electric short circuit could be detected, and then suspend the feeding movement of the tool electrode by the controlling system. The number of electric short circuit occurred during the EMM has been calculated to evaluate the machining stability. Obviously, the machining stability is in

Fig. 8 The scanning electron microscopy (SEM) image of the tool electrode used for electrochemical micromachining

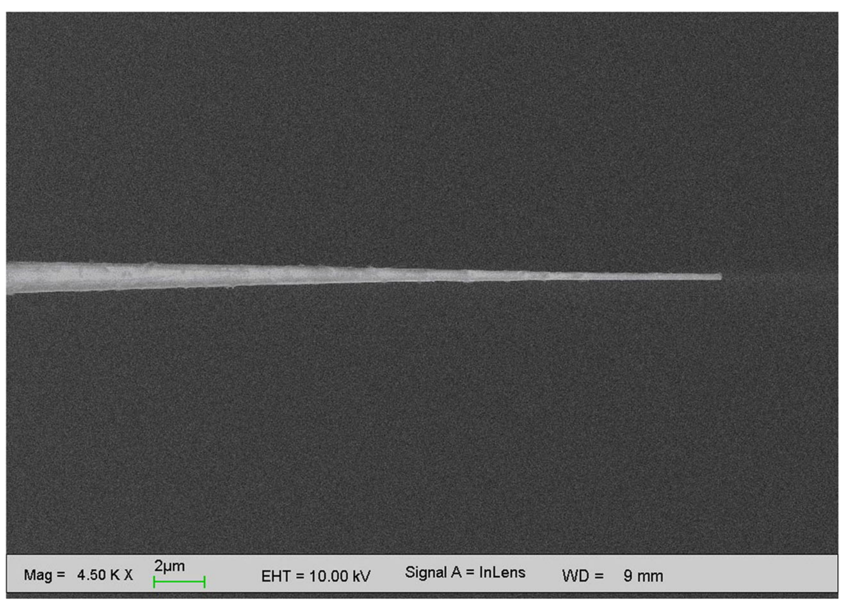

Table 1 Experimental conditions for electrochemical micromachining

Parameter	Value
Pulse voltage	4 V
Pulse duration	45 ns
Pulse period	500 ns
Electrolyte	0.1 M H_2SO_4
Tool diameter	0.65 μm
Workpiece size	10 × 10 × 1 mm
Temperature	24 °C

reverse proportional to the number of electric short circuit occurred during the EMM process.

4 Results and discussions

4.1 Effects of the workpiece oscillating amplitude

Figure 10 shows the microgrooves fabricated by EMM, with the varying amplitude of the oscillating workpiece. An initial interelectrode gap of 1 μm was set before the tool electrode move in the lateral directions with a programmed path and feeding rate. The tool electrode was scanned at the machining area in linear motion with a feeding rate of 0.2 μm/s, and a workpiece oscillating frequency of 50 Hz. The workpiece was oscillated with the amplitude of 0.1 μm, 0.3 μm, 0.5 μm, and 0.7 μm. An oscillating amplitude of larger than 0.7 μm was not used, in case of physical contact between the tool electrode tip and the workpiece. The width of the microgrooves increased with increasing vibrating amplitude. The side gap increased with the increasing oscillating amplitude, while the number of electric short circuit occurred during EMM decreased, as shown in Fig. 11. Thus, the machining stability of EMM could be enhanced with the larger oscillating amplitude.

As explained by Eqs. 7 and 12, both the material removal rate and the pressure in the interelectrode gap increase with the increasing oscillating workpiece amplitude. Because the absolute pressure between the tool electrode and workpiece increased with increasing amplitude, as shown in Fig. 5, the mass transport in the machining area could be enhanced with greater pressure variation under the flow of the electrolyte induced by the pressure gradient. And, the electrolyte in the machining area could be refreshed much efficiently arisen from the pressure gradient. Therefore, the machining stability could be improved with larger oscillating amplitude, due to the enhanced mass transport rates in the interelectrode gap. Furthermore, it was also revealed that the machining current increased during EMM with the increasing vibrating amplitude of the workpiece, as shown in Fig. 12. Therefore, the material removal rate and machining side gap increased with a larger vibrating amplitude, based on the Faraday's law.

The achievable maximum feeding rate of the tool obtained with the different vibrating amplitude of the workpiece was studied with experimental conditions listed in Table 1. It has been demonstrated that the maximum feeding rate could be improved with the larger amplitude, as shown in Fig. 13. Then, the machining efficiency could be increased by raising the vibrating amplitude of the workpiece. The maximum tool electrode feeding rate increased 200% when the vibrating amplitude increased from 0.1 to 0.7 μm. With a higher tool electrode feeding rate, microstructures with particular profiles could be processed in less time; thus, the machining efficiency could be improved.

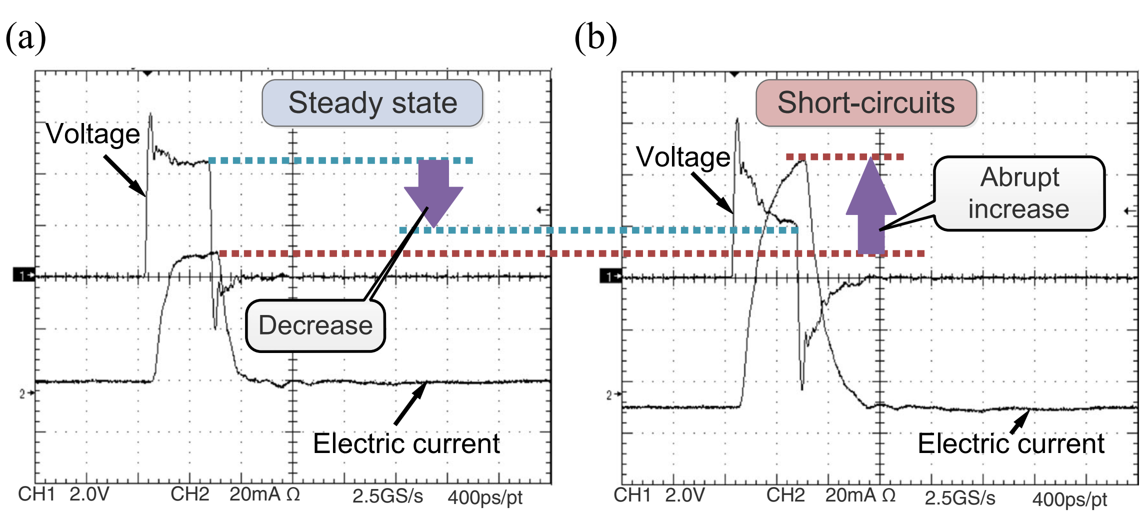

Fig. 9 The voltage and electric current signal between the workpiece and the tool electrode during the EMM process. The voltage and electric current signals at the steady state of EMM (**a**), an electric short circuit occurred while the tool electrode end touched with the workpiece (**b**)

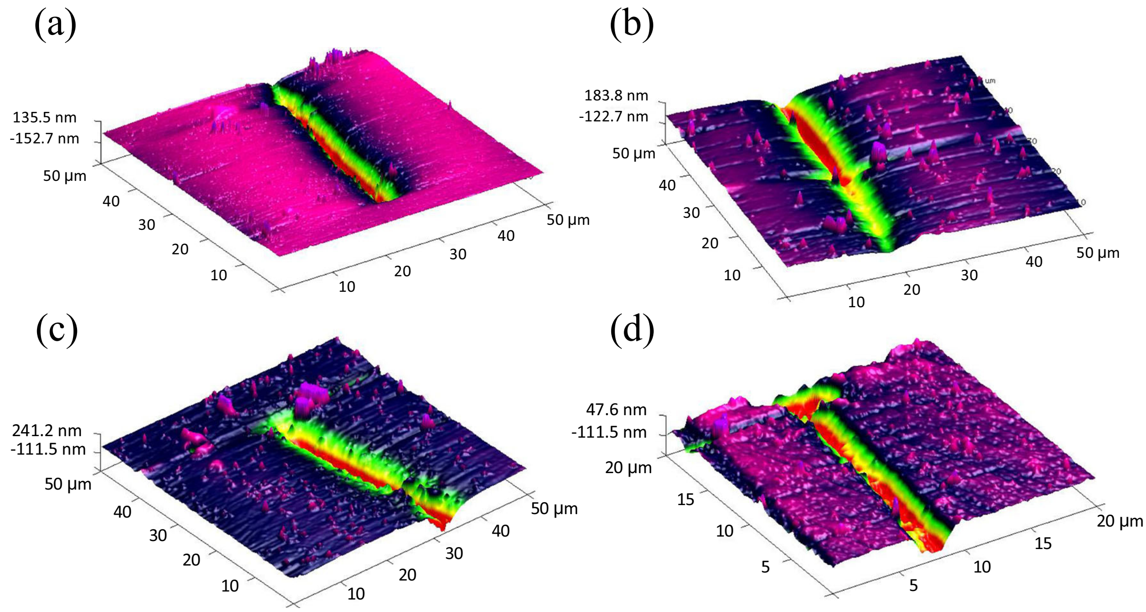

Fig. 10 AFM images of the microgrooves processed by EMM with the oscillating workpiece with a frequency of 50 Hz, and the oscillating amplitude of 0.1 μm (**a**), 0.3 μm (**b**), 0.5 μm (**c**), and 0.7 μm (**d**)

4.2 Effects of the workpiece vibrating frequency

The influences of vibrating frequency on the machining side gap and the machining stability were also studied. A workpiece vibrating amplitude of 0.5 μm was utilized. Figure 14 shows the microgrooves processed with the workpiece vibrating frequency of 0 Hz, 20 Hz, 60 Hz, and 100 Hz. It was revealed that the number of electric short circuit decreased with increasing vibrating frequency; thus, the machining stability was improved, as shown in Fig. 15. It was also observed that the machining side gap at the vibrating frequency of 60 Hz was the largest. Accordingly, the machining current also became the largest at the frequency about 60 Hz, based on the Faraday's law, as shown in Fig. 16. Because the material removal rate increases with the electric current density, the side gap increases with increasing vibrating frequency with the frequency smaller than 60 Hz.

As the above analysis in Section 2, the material removal rate and the mass transport in the interelectrode gap could be enhanced with the higher vibrating frequency.

Fig. 11 Variation of the machining side gap and the number of electric short circuit occurred during EMM with a workpiece vibrating amplitude

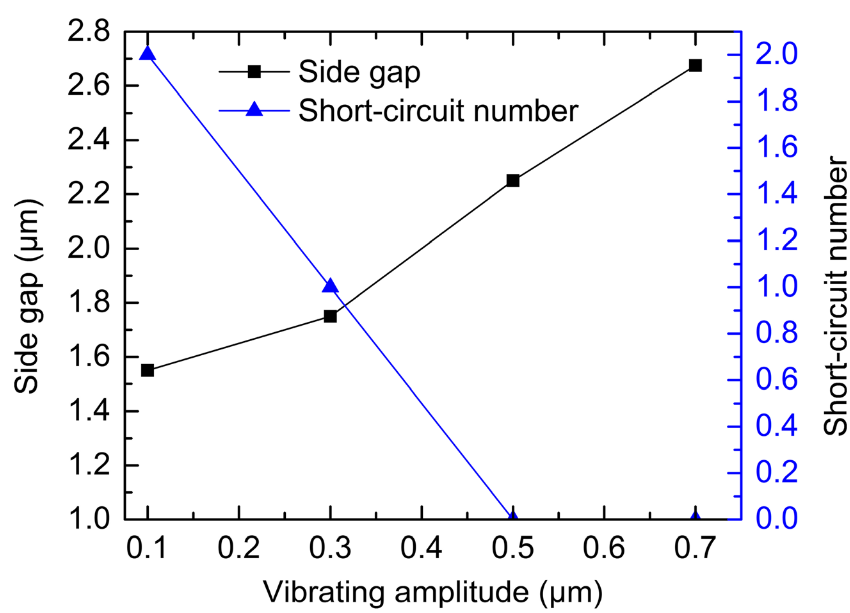

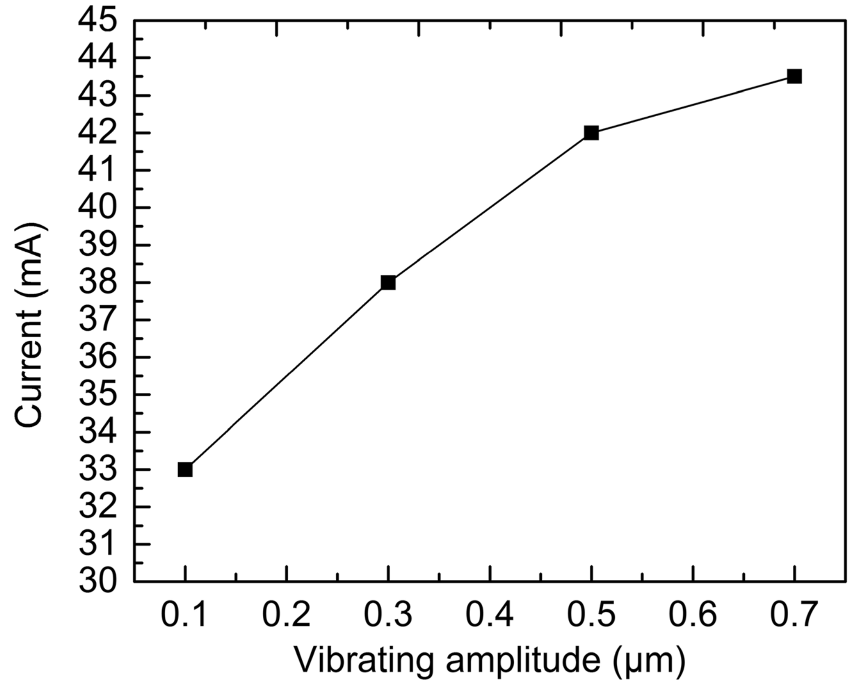

Fig. 12 Variation of the machining current during EMM with a vibrating amplitude

Also, the vibrating of the workpiece is beneficial to strengthen the exchange rate of the electrolytic ions at the interface of the electrolyte and electrode, which could improve the electric current densities in the machining area. Thus, the machining current and machining efficiency could be improved by increasing vibrating frequency of the tool electrode. However, as the vibrating frequency is larger than a threshold of about 60 Hz, a film of microbubbles may be formed at the workpiece surface, which could hinder the exchange of the electrolytic ions [21]. Therefore, the vibrating frequency of 60 Hz is recommended for improving the machining efficiency. Likewise, the achievable maximum feeding rate of the tool electrode was obtained at the vibrating frequency of 60 Hz, as shown in Fig. 17. The machining efficiency and side gap have been increased by 150% and 109% respectively with the oscillating frequency of 60 Hz compared with that without oscillation introduced to the workpiece.

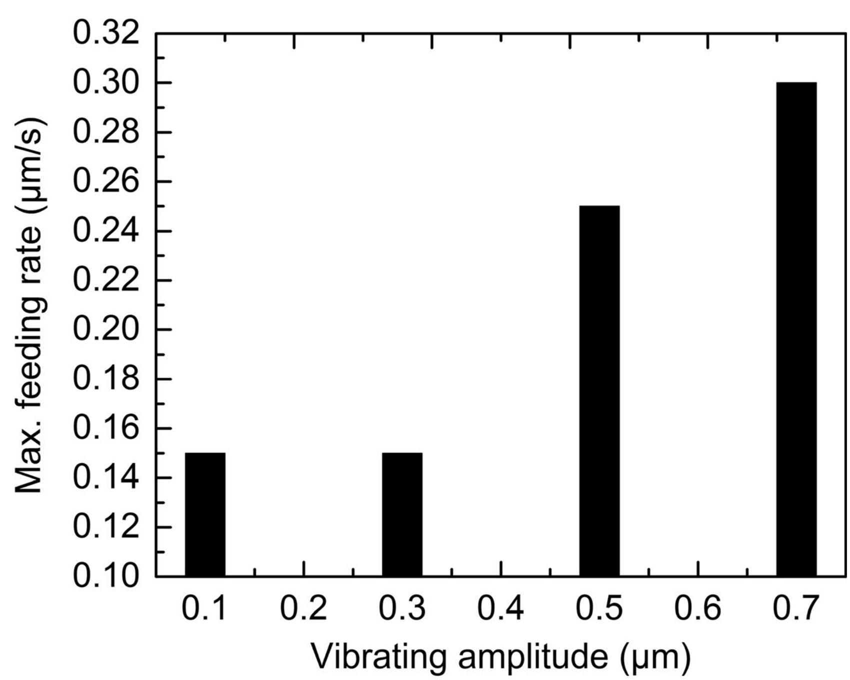

Fig. 13 Variation of the achievable maximum feeding rate of the tool electrode during EMM with a vibrating amplitude of the workpiece

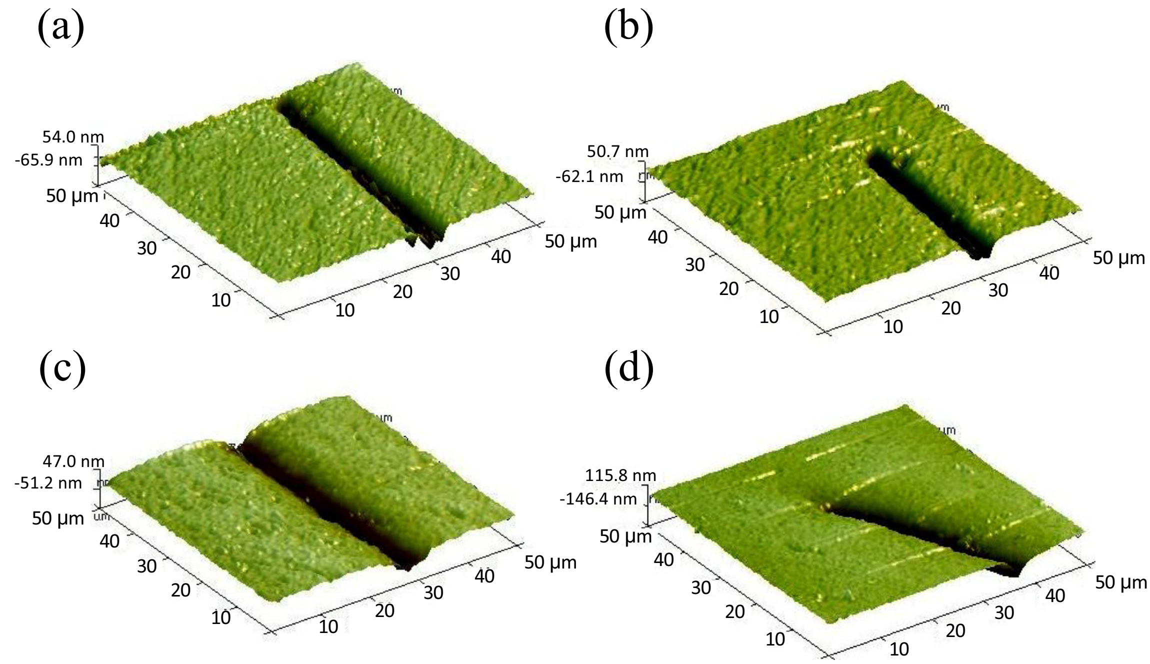

Fig. 14 AFM images of the microgrooves processed by EMM with the oscillating workpiece with an amplitude of 0.5 μm and vibrating frequency of 0 Hz (**a**), 20 Hz (**b**), 60 Hz (**c**), and 100 Hz (**d**)

4.3 Processing of the microstructures with controlled profiles

A higher vibrating amplitude and the proper frequency of about 60 Hz were preferred to improve the machining efficiency and stability. Thus, a greater feeding rate could be utilized by the tool electrode during EMM with optimum experimental conditions. A higher feeding rate could contribute to improving the machining precision. Figure 18 shows the processed microstructures with circular profiles, by controlling the moving trajectory of the workpiece (Fig. 18b). A vibrating amplitude of 0.5 μm, frequency of 60 Hz, and tool feeding rate of 0.3 μm/s were used. The machining side gap was 0.675 μm. During the whole machining process, no electric short circuit has been detected.

5 Conclusions

Electrochemical micromachining utilizing the oscillating workpiece has been studied to enhance the machining

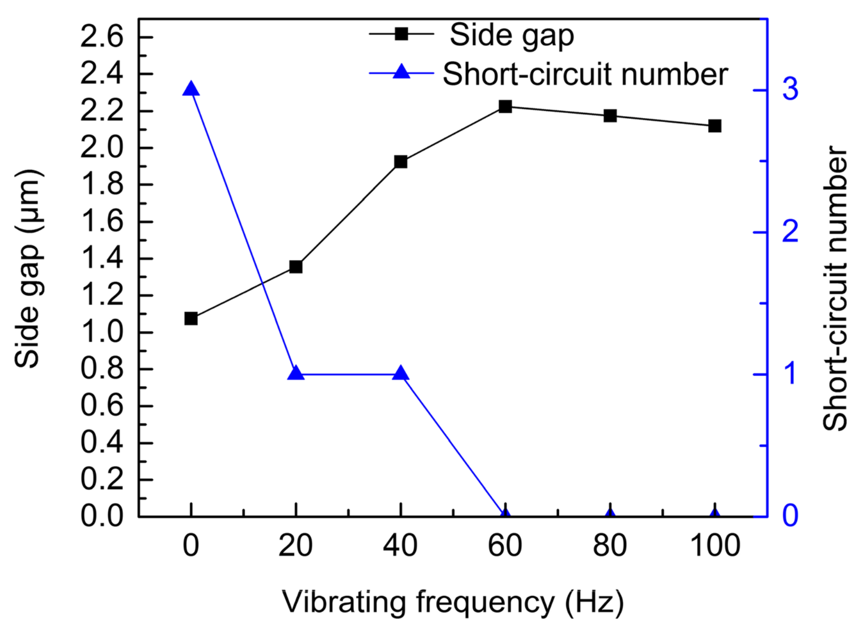

Fig. 15 Variation of the machining side gap and number of electric short circuit occurred during EMM with vibrating frequency

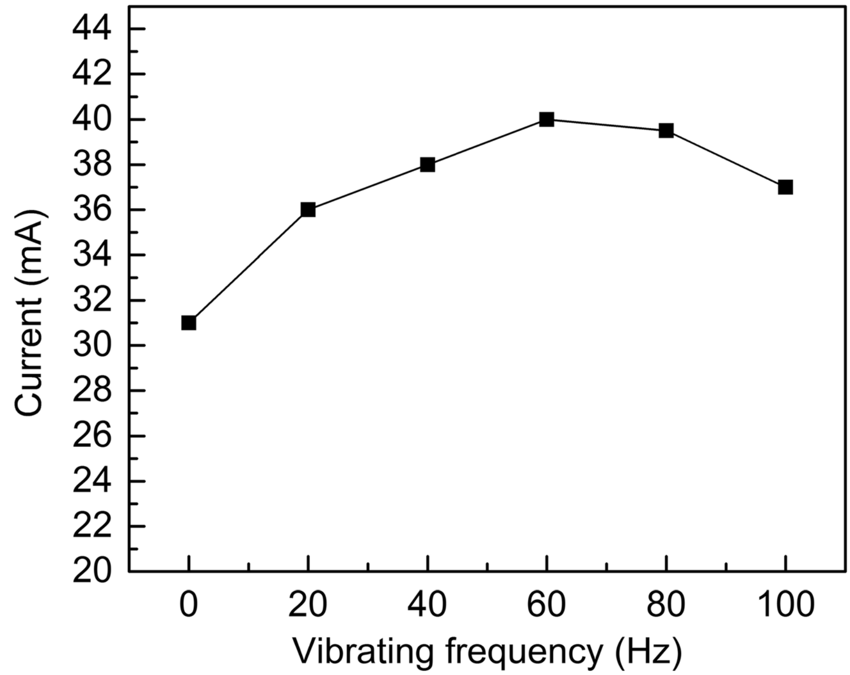

Fig. 16 Variation of machining current during EMM with vibrating frequency

efficiency and stability. The main conclusions can be drawn as follows:

(1) Mathematical models for the material removal rate and the pressure in the interelectrode gap during the EMM were derived. The influences of workpiece oscillating parameters on the material removal rate and the pressure in the interelectrode gap were studied theoretically.
(2) The mechanisms of enhancing the mass transport in the interelectrode gap induced by the workpiece oscillation during EMM have been analyzed.
(3) Experiments have been conducted to investigate the influences of a workpiece vibrating amplitude and frequency on the machining efficiency, stability, and achievable maximum feeding rate of the tool electrode. The results indicated that a larger vibrating amplitude and proper frequency of about 60 Hz were suitable for increasing

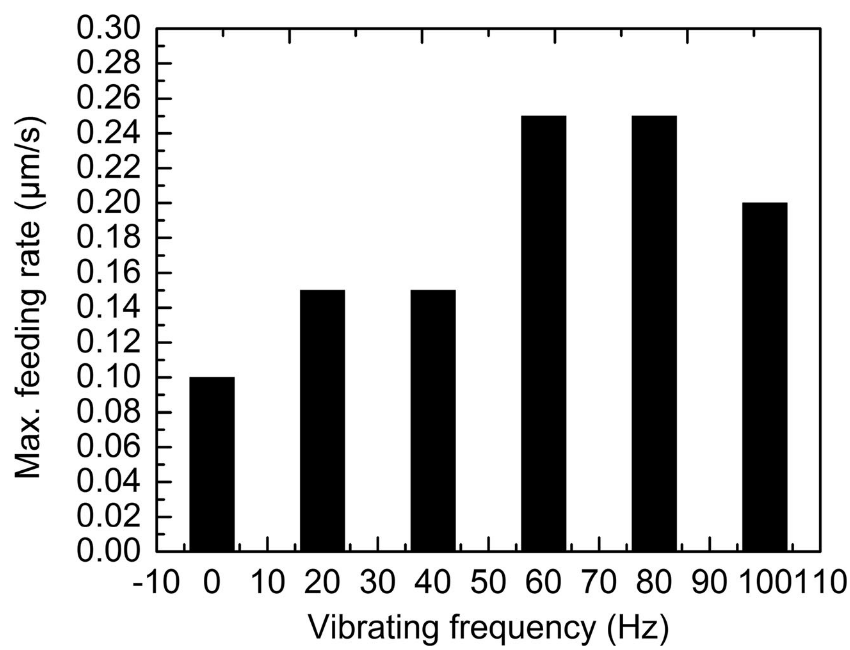

Fig. 17 Variation of the maximum achievable feeding rate of the tool electrode during EMM with vibrating frequency of the workpiece

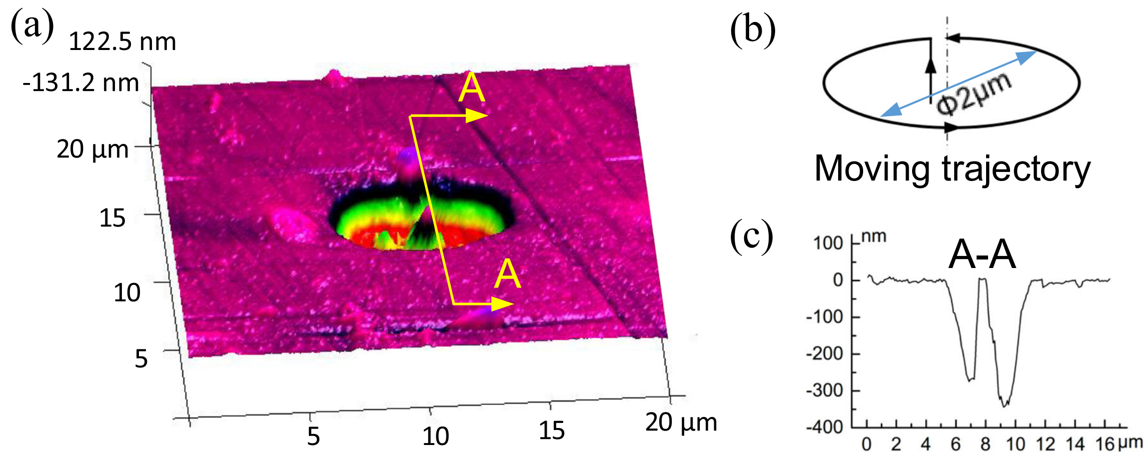

Fig. 18 The processed microstructure using EMM assisted by oscillating workpiece, microstructures with circular profiles (**a**), the moving trajectory of the workpiece (**b**), and the cross-sectional contour of the microstructure (**c**)

machining efficiency of EMM. The highest feeding rate of 0.3 μm/s has been obtained utilizing oscillating workpiece during EMM. An increase of 150% and 109% in the machining efficiency and side gap was obtained with the oscillating frequency of 60 Hz compared with that without oscillation introduced to the workpiece.

(4) Microstructures with the controlled profiles could be processed by controlling the trajectory of the sub-micro scale tool electrode with the oscillating workpiece with tool feeding rate of 0.3 μm/s, which has been improved by 15.4% compared with the previous study in which the tool electrode vibrated in EMM [21].

Funding information This work was financially supported by China Postdoctoral Science Foundation (2017M621983) and Zhejiang Provincial Natural Science Foundation (LQ19E050003).

Publisher's note Springer Nature remains neutral with regard to jurisdictional claims in published maps and institutional affiliations.

References

1. Lee ES, Baek SY, Cho CR (2007) A study of the characteristics for electrochemical micromachining with ultrashort voltage pulses. Int J Adv Manuf Technol 31:762–769
2. Rajurkar KP, Levy G, Malshe A, Sundaram MM, McGeough J, Hu X, Resnick R, DeSilva A (2006) Micro and nano machining by electro-physical and chemical processes. CIRP Ann - Manuf Technol 55:643–666
3. Schuster R, Kirchner V, Allongue P, Ertl G (2000) Electrochemical micromachining. Science 289:98–101
4. Kock M, Kirchner V, Schuster R (2003) Electrochemical micromachining with ultrashort voltage pulses – a versatile method with lithographical precision. Electrochim Acta 48:3213–3219
5. Ahn SH, Shi HR, Choi DK, Chu CN (2004) Electro-chemical micro drilling using ultra short pulses. Precis Eng 28:129–134
6. Kim BH, Ryu SH, Choi DK, Chu CN (2005) Micro electrochemical milling. J Micromech Microeng 15:124–129
7. Liu Y, Zhu D, Zhu L (2012) Micro electrochemical milling of complex structures by using in situ fabricated cylindrical electrode. Int J Adv Manuf Technol 60:977–984
8. Mithu MAH, Fantoni G, Ciampi J (2011) The effect of high frequency and duty cycle in electrochemical microdrilling. Int J Adv Manuf Technol 55:921–933
9. Ghoshal B, Bhattacharyya B (2015) Investigation on profile of microchannel generated by electrochemical micromachining. J Mater Process Technol 222:410–421
10. Ghoshal B, Bhattacharyya B (2013) Influence of vibration on micro-tool fabrication by electrochemical machining. Int J Mach Tools Manuf 64:49–59
11. Rathod V, Doloi B, Bhattacharyya B (2015) Influence of electrochemical micromachining parameters during generation of microgrooves. Int J Adv Manuf Technol 76:51–60
12. Ebeid SJ, Hewidy MS, El-Taweel TA, Youssef AH (2004) Towards higher accuracy for ECM hybridized with low-frequency vibrations using the response surface methodology. J Mater Process Technol 149:432–438
13. Munda J, Malapati M, Bhattacharyya B (2007) Control of microspark and stray-current effect during EMM process. J Mater Process Technol 194:151–158
14. Bhattacharyya B, Malapati M, Munda J, Sarkar A (2007) Influence of tool vibration on machining performance in electrochemical micro-machining of copper. Int J Mach Tools Manuf 47:335–342
15. Hewidy MS, Ebeid SJ, El-Taweel TA, Youssef AH (2007) Modelling the performance of ECM assisted by low frequency vibrations. J Mater Process Technol 189:466–472
16. Yang I, Park MS, Chu CN (2009) Micro ECM with ultrasonic vibrations using a semi-cylindrical tool. Int J Precis Eng Manuf 10:5–10
17. Zeng YB, Yu Q, Wang SH, Zhu D (2012) Enhancement of mass transport in micro wire electrochemical machining. CIRP Ann-Manuf Technol 61:195–198
18. Natsu W, Nakayama H, Yu Z (2012) Improvement of ECM characteristics by applying ultrasonic vibration. Int J Precis Eng Manuf 13:1131–1136
19. Xu L, Pan Y (2014) Electrochemical micromachining using vibrating tool electrode. Int J Adv Manuf Technol 75:645–650
20. Wang S, Zhu D, Zeng Y, Liu Y (2011) Micro wire electrode electrochemical cutting with low frequency and small amplitude tool vibration. Int J Adv Manuf Technol 53:535–544

21. Ghoshal B, Bhattacharyya B (2015) Vibration assisted electrochemical micromachining of high aspect ratio micro features. Precis Eng 42:231–241
22. Wang MH, Zhang Y, He Z, Peng W (2016) Deep micro-hole fabrication in EMM on stainless steel using disk micro-tool assisted by ultrasonic vibration. J Mater Process Technol 229:475–483
23. Ghoshal B, Bhattacharyya B (2014) Shape control in micro borehole generation by EMM with the assistance of vibration of tool. Precis Eng 38:127–137
24. Fan ZW, Hourng LW (2011) Electrochemical micro-drilling of deep holes by rotational cathode tools. Int J Adv Manuf Technol 52:555–563
25. Zhao WS, Wang ZL, Di S, Chi G, Wei Y (2002) Ultrasonic and electric discharge machining to deep and small hole on titanium alloy. J Mater Process Technol 120:101–106
26. Wang Y, Zeng Y, Qu N, Zhu D (2015) Electrochemical etching of cylindrical nanoprobes using a vibrating electrolyte. Rev Sci Instrum 86:076103